On the Dynamics of Bounding and Extensions: Towards the Half-Bound and Gallop Gaits

Ioannis Poulakakis, James Andrew Smith, and Martin Buehler

Ambulatory Robotics Laboratory, Centre for Intelligent Machines,
McGill University, Montréal QC H3A 2A7, Canada

Abstract. This paper examines how simple control laws stabilize complex running behaviors such as bounding. First, we discuss the unexpectedly different local and global forward speed versus touchdown angle relationships in the self-stabilized Spring Loaded Inverted Pendulum. Then we show that, even for a more complex energy conserving unactuated quadrupedal model, many bounding motions exist, which can be locally open loop stable! The success of simple bounding controllers motivated the use of similar control laws for asymmetric gaits resulting in the first experimental implementations of the half-bound and the rotary gallop on Scout II.

1 Introduction

Many mobile robotic applications might benefit from the improved mobility and versatility of legs. Twenty years ago, Raibert set the stage with his groundbreaking work on dynamically stable legged robots by introducing a simple and highly effective three-part controller for stabilizing running on his one-, two-, and four-legged robots, [9]. Other research showed that even simpler control laws, which do not require task level or body state feedback, can stabilize running as well, [1]. Previous work on the Scout II quadruped (Fig. 1) showed that *open loop* control laws simply positioning the legs at a desired touchdown angle, result in stable running at speeds over 1 m/s, [12].

Fig. 1. Scout II: A simple four-legged robot.

Motivated by experiments on cockroaches (death-head cockroach, *Blaberous discoidalis*), Kubow and Full studied the role of the mechanical system in control by developing a simple two-dimensional hexapedal model, [5]. The model included no equivalent of nervous feedback and it was found to

be inherently stable. This work first revealed the significance of mechanical feedback in simplifying neural control. Full and Koditschek set a foundation for a systematic study of legged locomotion by introducing the concepts of *templates* and *anchors*, [2]. To study the basic properties of sagittal plane running, the *Spring Loaded Inverted Pendulum (SLIP)* template has been proposed, which describes running in animals that differ in skeletal type, leg number and posture, [2]. Seyfarth et al., [11], and Ghigliazza et al., [3], found that for certain leg touchdown angles, the SLIP becomes self-stabilized if the leg stiffness is properly adjusted and a minimum running speed is exceeded.

In this paper, we first describe some interesting aspects of the relationship between forward speed and leg touchdown angles in the self-stabilized SLIP. Next, we attempt to provide an explanation for simple control laws being adequate in stabilizing complex tasks such as bounding, based on a simple sagittal "template" model. Passively generated cyclic bounding motions are identified and a regime where the system is self-stabilized is also found. Furthermore, motivated by the success of simple control laws to generating bounding running, we extended the bounding controller presented in [12] to allow for asymmetric three- and four-beat gaits. The half-bound, [4], and the rotary gallop [4,10], expand our robots' gait repertoire, by introducing an asymmetry to the bound, in the form of the leading and trailing legs. To the authors' best knowledge this is the first implementation of both the half-bound and the gallop in a robot.

2 Bounding experiments with Scout II

Scout II (Fig. 1) has been designed for power-autonomous operation. One of its most important features is that it uses a *single* actuator per leg. Thus, each leg has two degrees of freedom (DOF): the actuated revolute hip DOF, and the passive linear compliant leg DOF.

In the bound gait the essential components of the motion take place in the sagittal plane. In [12] we propose a controller, which results in fast and robust bounding running with forward speeds up to 1.3 m/s, without body state feedback. The controller is based on two individual, independent front and back virtual leg controllers. The front and back virtual legs each detect two leg states - stance and flight. During flight, the controller servoes the flight leg to a desired, fixed, touchdown angle. During stance the leg is swept back with a constant commanded torque until a sweep limit is reached. Note that the actual applied torque during stance is determined primarily by the motor's torque-speed limits, [12]. The sequence of the phases of the resulting bounding gait is given in Fig. 2.

Scout II is an underactuated, highly nonlinear, intermittent dynamic system. The limited ability in applying hip torques due to actuator and friction constraints and due to unilateral ground forces further increases the complexity. Furthermore, as Full and Koditschek state in [2], "locomotion results from

complex high-dimensional, dynamically coupled interaction between an organism and its environment". Thus, the task itself is complex too, and cannot be specified via reference trajectories. Despite this complexity, simple control laws, like the one described above and in [12], can stabilize periodic motions, resulting in robust and fast running without requiring any task level feedback like forward velocity. Moreover, they do not require body state feedback.

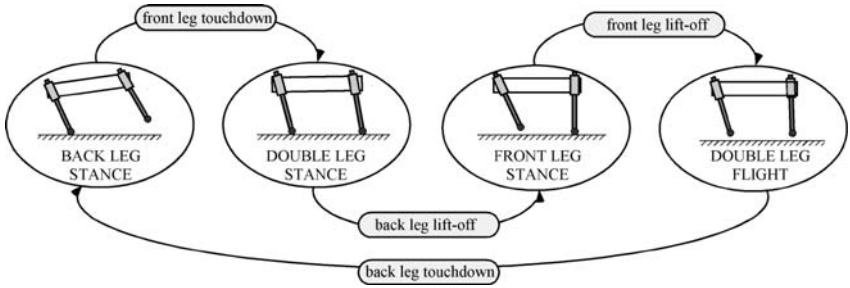

Fig. 2. Bounding phases and events.

It is therefore natural to ask why such a complex system can accomplish such a complex task without intense control action. As outlined in this paper, and in more detail in [7,8], a possible answer is that Scout II's unactuated, conservative dynamics already exhibit stable bounding cycles, and hence a simple controller is all that is needed for keeping the robot bounding.

3 Self-stabilization in the SLIP

The existence of passivelly stable gaits in the conservative, unactuated SLIP, discussed in [3,11], is a celebrated result that suggests the significance of the mechanical system in control as was first pointed out by Kubow and Full in [5]. However, the mechanism that results in self-stabilization is not yet fully understood, at least in a way that could immediately be applicable to improve existing control algorithms. It is known that for a set of initial conditions (forward speed and apex height), there exists a touchdown angle at which the system maintains its initial forward speed, see Fig. 3 (left). As Raibert noticed, [9], if these conditions are perturbed, for example, by decreasing the touchdown angle, then the system will accelerate in the first step, and, if the touchdown angle is kept constant, it will also accelerate in the subsequent steps and finally fall due to toe stubbing. However, when the parameters are within the self-stabilization regime, the system does not fall! It converges to a periodic motion with symmetric stance phases and higher forward speeds. This fact is not captured in Raibert's linear steady-state argument, [9], based on which one would be unable to predict self-stabilization of the system.

A question we address next is what is the relationship between the forward speed at which the system converges i.e. *the speed at convergence*, and the touchdown angle. To this end, simulation runs have been performed in which

the initial apex height and initial forward velocity are fixed, thus the energy level is fixed, while the touchdown angle changes in a range where cyclic motion is achieved. For a given energy level, this results in a curve relating the speed at convergence to the touchdown angle. Subsequently, the apex height is kept constant, while the initial forward velocity varies between 5 and 7 m/s. This results in a family of constant energy curves, which are plotted in Fig. 3 (right). It is interesting to see in Fig. 3 that in the self-stabilizing regime of the SLIP, an increase in the touchdown angle *at constant energy* results in a lower forward speed at convergence. This means that higher steady state forward speeds can be accommodated by smaller touchdown angles, which, at first glance, is not in agreement with the *global* behavior that higher speeds require bigger (flatter) touchdown angles and is evident in Fig. 3 (right).

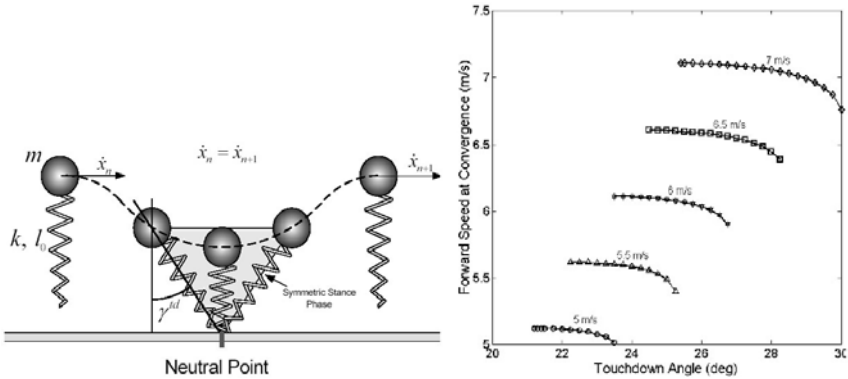

Fig. 3. Left: Symmetric stance phase in the SLIP. Right: Forward speed at convergence versus touchdown angle at fixed points obtained for initial forward speeds 5 to 7 m/s and apex height equal to 1 m (l_0 =1 m, k =20 kN/m and m =1 kg).

The fact that *globally* fixed points at higher speeds require greater (flatter) touchdown angles was reported by Raibert and it was used to control the speed of his robots based on a feedback control law, [9]. However, Fig. 3 (right) suggests that in the *absence* of control and for *constant energy*, reducing the touchdown angle results in an increase of the speed at convergence. Thus, one must be careful not to transfer results from systems actively stabilized to passive systems, because otherwise opposite outcomes from those expected may result. Note also that there might exist parameter values resulting in a local behavior opposite to that in Fig. 3, illustrating that direct application of the above results in designing intuitive controllers is not trivial.

4 Modeling the Bounding Gait

In this section the passive dynamics of Scout II in bounding is studied based on the template model shown in Fig. 4 and conditions allowing steady state cyclic motion are determined.

Assuming that the legs are massless and treating toes in contact with the ground as frictionless pin joints, the equations of motion for each phase are

$$\frac{d}{dt}\begin{bmatrix}\mathbf{q}\\ \dot{\mathbf{q}}\end{bmatrix} = \begin{bmatrix}\dot{\mathbf{q}}\\ -\mathbf{M}^{-1}\left(\mathbf{F_{el}}+\mathbf{G}\right)\end{bmatrix}, \tag{1}$$

where $\mathbf{q} = [x\, y\, \theta]^T$ (Fig. 4), $\mathbf{M}$, is the mass matrix and $\mathbf{F_{el}}$, $\mathbf{G}$ are the vectors of the elastic and gravitational forces, respectively. The transition conditions between phases corresponding to touchdown and lift-off events are

$$y \pm L\sin\theta \leq l_0 \cos\gamma_i^{td}, \;\; l_i \leq l_0, \tag{2}$$

where $i = b,\, f$ for the back (- in (2)) and front (+ in (2)) leg respectively.

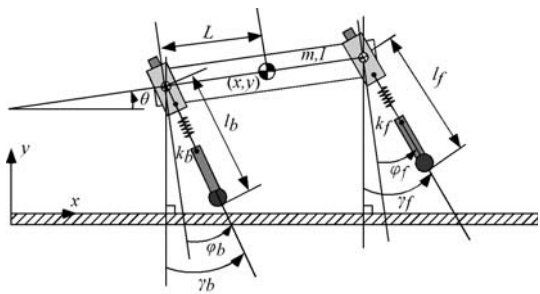

Fig. 4. A template for studying sagittal plane running.

To study the bounding cycle of Fig. 2 a return map is defined using the apex height in the double leg flight phase as a reference point. The states at the n^{th} apex height constitute the initial conditions for the cycle, based on which we integrate successively the dynamic equations of all the phases. This process yields the state vector at the $(n+1)^{th}$ apex height, which is the value of the return map $\mathbf{P} : \Re^4 \times \Re^2 \rightarrow \Re^4$ calculated at the n^{th} apex height, i.e.

$$\mathbf{x}_{n+1} = \mathbf{P}(\mathbf{x}_n, \mathbf{u}_n), \tag{3}$$

with $\mathbf{x} = [y\ \theta\ \dot{x}\ \dot{\theta}]^T$, $\mathbf{u} = [\gamma_b^{td}\ \gamma_f^{td}]^T$; the touchdown angles are control inputs.

We seek conditions that result in cyclic motion and correspond to fixed points $\bar{\mathbf{x}}$ of $\mathbf{P}$, which can be determined by solving $\mathbf{x} - \mathbf{P}(\mathbf{x}) = \mathbf{0}$ for all the (experimentally) reasonable touchdown angles. The search space is 4-dimensional with two free parameters and the search is conducted using the Newton-Raphson method. An initial guess, $\mathbf{x}_n^{\langle 0\rangle}$, for a fixed point is updated by

$$\mathbf{x}_n^{\langle k+1\rangle} = \mathbf{x}_n^{\langle k\rangle} + \left(\mathbf{I} - \nabla\mathbf{P}\left(\mathbf{x}_n^{\langle k\rangle}\right)\right)^{-1}\left[\mathbf{P}\left(\mathbf{x}_n^{\langle k\rangle}\right) - \mathbf{x}_n^{\langle k\rangle}\right], \tag{4}$$

where n corresponds to the n^{th} apex height and k to the number of iterations. Evaluation of (4) until convergence (the error between $\mathbf{x}_n^{\langle k\rangle}$ and $\mathbf{x}_n^{\langle k+1\rangle}$ is smaller than $1e{-}6$) yields the solution. To calculate $\mathbf{P}$ at $\mathbf{x}_n^{\langle k\rangle}$, we numerically integrate (1) for each phase using the adaptive step Dormand-Price method with $1e-6$ and $1e-7$ relative and absolute tolerances, respectively.

Implementation of (4) resulted in a large number of fixed points of $\mathbf{P}$, for different initial guesses and touchdown angles, which exhibited some very useful properties, [7,8]. For instance, the pitch angle was found to be always zero at the apex height. More importantly, the following condition was found to be true for all the fixed points calculated randomly using (4)

$$\gamma_f^{td} = -\gamma_b^{lo},\ \gamma_b^{td} = -\gamma_f^{lo}. \tag{5}$$

It is important to mention that this property resembles the case of the SLIP, in which the condition for fixed points is the lift-off angle to be equal to the negative of the touchdown angle (symmetric stance phase), [3].

It is desired to find fixed points at specific forward speeds and apex heights. Therefore, the search scheme described above is modified so that the forward speed and apex height become its input parameters, specified according to running requirements, while the touchdown angles are now considered to be "states" of the search procedure, i.e. variables to be determined from it, [7,8]. Thus, the *search space* states and the "inputs" to the search scheme are $\mathbf{x}^* = [\theta\ \dot{\theta}\ \gamma_b^{td}\ \gamma_f^{td}]^T$ and $\mathbf{u}^* = [y\ \dot{x}]^T$, respectively.

Fig. 5 illustrates that for 1 m/s forward speed, 0.35 m apex height and varying pitch rate there is a continuum of fixed points, which follows an "eye" pattern accompanied by two external branches. The existence of the external branch implies that there is a range of pitch rates where two *different* fixed points exist for the same forward speed, apex height and pitch rate. This is surprising since the same total energy and the same distribution of that energy among the three modes of the motion -forward, vertical and pitch- can result in two different motions depending on the touchdown angles. Fixed points that lie on the internal branch correspond to a bounding motion where the front leg is brought in front of the torso, while fixed points that lie on the external branch correspond to a motion where the front leg is brought towards the torso's Center of Mass (COM), see Fig. 5 (right).

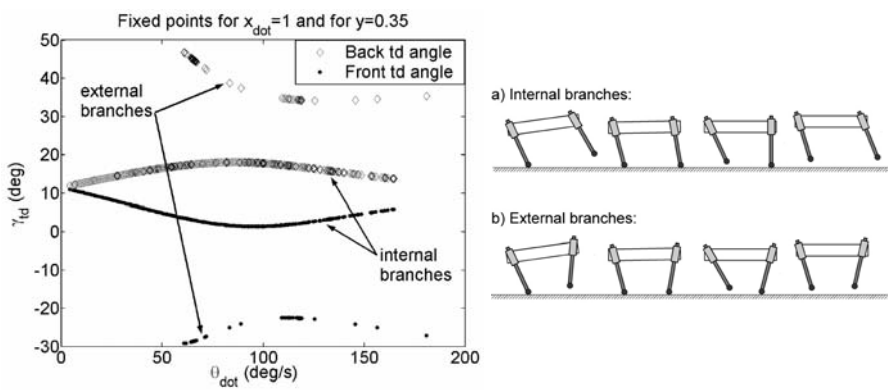

Fig. 5. Left: Fixed points for 1m/s forward speed and 0.35 m apex height. Right: Snapshots showing the corresponding motions.

5 Local stability of passive bounding

The fact that bounding cycles can be generated passively as a response to the appropriate initial conditions may have significant implications for control. Indeed, if the system remains close to its passive behavior, then the actuators have less work to do to maintain the motion and energy efficiency, an important issue to any mobile robot, is improved. Most importantly there might exist operating regimes where the system is passively stable, thus active stabilization will require less control effort and sensing. The local stability of the fixed points found in the previous section is now examined. A periodic solution corresponding to a fixed point $\bar{\mathbf{x}}$ is stable if all the eigenvalues of the matrix $\mathbf{A} = \partial \mathbf{P}(\mathbf{x}, \mathbf{u})/\partial \mathbf{x}|_{\mathbf{x}=\bar{\mathbf{x}}}$ have magnitude less than one.

Fig. 6 (left) shows the eigenvalues of $\mathbf{A}$ for forward speed 1 m/s, apex height 0.35 m and varying pitch rate, $\dot{\theta}$. The four eigenvalues start at dark reqions (small $\dot{\theta}$), move along the directions of the arrows and converge to the points marked with "x" located in the brighter regions (large $\dot{\theta}$) of the root locus. One of the eigenvalues (#1) is always located at one, reflecting the conservative nature of the system. Two of the eigenvalues (#2 and #3) start on the real axis and as $\dot{\theta}$ increases they move towards each other, they meet inside the unit circle and then move towards its rim. The fourth eigenvalue (#4) starts at a high value and moves towards the unit circle but it never gets into it, for those specific values of forward speed and apex height. Thus, the system cannot be passively stable for these parameter values.

To illustrate how the forward speed affects stability we present Fig. 6 (right), which shows the magnitude of the larger eigenvalue (#4) at two different forward speeds. For sufficiently high forward speeds and pitch rates, the larger eigenvalue enters the unit circle while the other eigenvalues remain well behaved. Therefore, there exists a regime where the system can be passively stable. This is a very important result since it shows that the system can tolerate perturbations of the nominal conditions without any control action taken! This fact could provide a possible explanation to why Scout II can bound without the need of complex state feedback controllers. It is important to mention that this result is in agreement with recent research from biomechanics, which shows that when animals run at high speeds, passive dynamic self-stabilization from a feed-forward, tuned mechanical system can reject rapid perturbations and simplify control, [2,3,5,11]. Analogous behavior has been discovered by McGeer in his passive bipedal running work, [6].

6 The half-bound and rotary gallop gaits

This section describes the half-bound and rotary gallop extensions to the bound gait. The controllers for both these gaits are generalizations of the original bounding controller, allowing two asymmetric states to be observed in the front lateral leg pair and adding control methods for these new states.

In the half-bound and rotary gallop controllers the lateral leg pair state machine adds two new asymmetric states: the left leg can be in flight while the

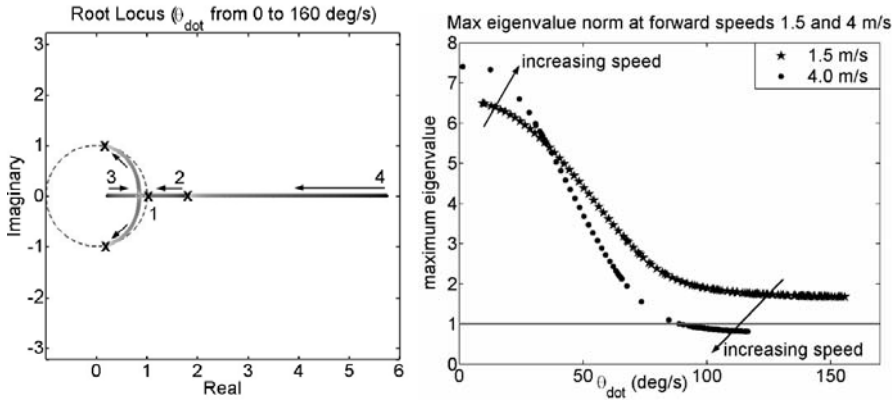

Fig. 6. Left: Root locus showing the paths of the four eigenvalues as the pitch rate, $\dot{\theta}$, increases. Right: Largest eigenvalue norm at various pitch rates and for forward speeds 1.5 and 4m/s. The apex height is 0.35 m.

right leg is in stance, and vice versa. In the regular bounding state machine these asymmetric states are ignored and state transitions only occur when the lateral leg pair is in the same state: either both in stance or both in flight. The control action associated with the asymmetric states enforces a phase difference between the two legs during each leg's flight phase, but is otherwise unchanged from the bounding controller as presented in [12].

The following describes the front leg control actions. Leg 1 (left) touches down before Leg 3 (right):

Case 1: Leg 1 and Leg 3 in flight. Leg 1 is actuated to a touchdown angle (17^o, with respect to the body's vertical). Leg 3 is actuated to a larger touchdown angle (32^o) to enforce separate touchdown times.

Case 2: Leg 1 and Leg 3 in stance. Constant commanded torques until 0^o.

Case 3: Leg 1 in stance, Leg 3 in flight. Leg 1 is commanded as in Case 2 and Leg 3 as in Case 1.

Case 4: Leg 1 in flight, Leg 3 in stance. Leg 1 is commanded as in Case 1 and Leg 3 as in Case 2.

Application of the half-bound controller results in the motion shown in Fig. 7; the front legs are actuated to the two separate touchdown angles and maintain an out-of-phase relationship during stance, while the back two legs have virtually no angular phase difference at any point during the motion. Application of the rotary gallop controller results in the motion in Fig. 8; the front and back leg pairs are actuated to out-of-phase touchdown angles (Leg 1: 17^o, Leg 3: 32^o, Leg 4: 17^o, Leg 2: 32^o).

Fig. 9 (left) illustrates the half-bound footfall pattern. The motion stabilizes approximately one second after it begins (at 132 s), without back leg phase difference. Fig. 9 (right) shows the four-beat footfall pattern for the rotary gallop. The major difference between both the bound and the half-

bound controllers and the gallop controller is that a phase difference of 15^o (Leg 4: 17^o; Leg 2: 32^o) is enforced between the two back legs during the double-flight phase. It must be mentioned here that although the half-bound and the rotary gallop gaits have been studied in biological systems [4], to the authors' best knowledge this is the first implementation on a robot.

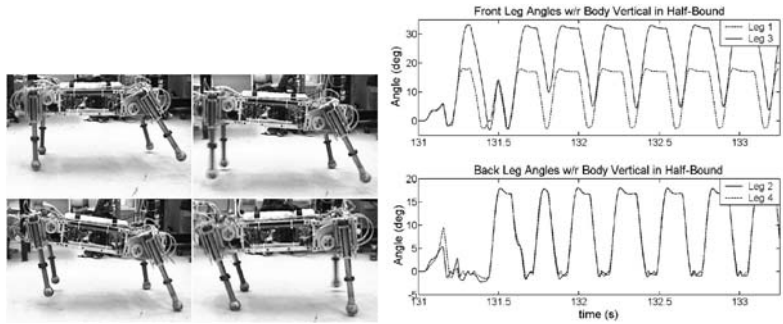

Fig. 7. Left: Snapshots of Scout II during the half bound: back legs (#2,4) in stance, front left leg (#1) touchdown, front right leg (#3) touchdown, and back legs (#2,4) touchdown. Right: Leg angles in the half-bound.

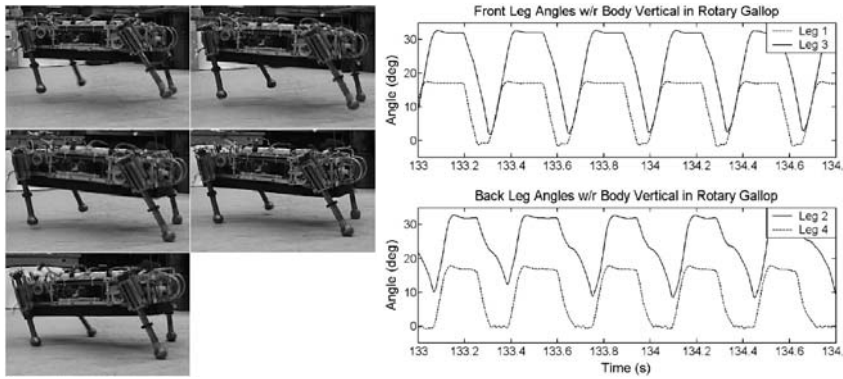

Fig. 8. Snapshots of Scout II during the rotary gallop: All legs in flight, first front leg (#1) touchdown, second front leg (#3) touchdown, first back leg (#4) touchdown and second back leg (#2) touchdown. Right: Leg angles in the rotary gallop.

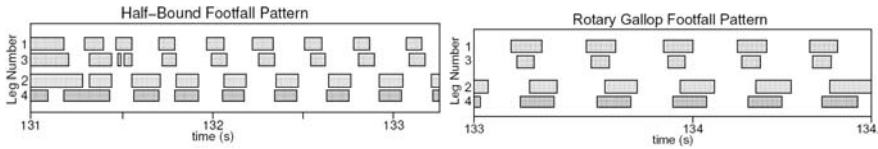

Fig. 9. Stance phases (shaded) for the half-bound (left) and rotary gallop (right).

7 Conclusion

This paper examined the difference between the local and global forward speed versus touchdown angle relationships in the self-stabilized SLIP. It then showed that a more complex model for quadruped sagittal plane running can exhibit passively generated bounding cycles under appropriate initial conditions. Most strikingly, under some initial conditions the model was found to be self-stable! This might explain why simple controllers as those in [12], are adequate in stabilizing a complex dynamic task like running. Self-stabilization can facilitate the control design for dynamic legged robots. Furthermore, preliminary experimental results of the half-bound and rotary gallop running gaits have been presented. Future work includes the application of asymmetric gaits to improving maneuverability on Scout II.

Acknowledgments

Support by IRIS III and by NSERC is gratefully acknowledged. The work of I. Poulakakis has been supported by a R. Tomlinson Doctoral Fellowship and by the Greville Smith McGill Major Scholarship.

References

1. Buehler M. 2002. Dynamic Locomotion with One, Four and Six-Legged Robots. *J. of the Robotics Society of Japan* 20(3):15-20.
2. Full R. J. and Koditschek D. 1999. Templates and Anchors: Neuromechanical Hypotheses of Legged Locomotion on Land. *J. Exp. Biol.* 202:3325-3332.
3. Ghigliazza R. M., Altendorfer R., Holmes P. and Koditschek D. E. 2003. A Simply Stabilized Running Model. *SIAM J. on Applied Dynamical Systems* 2(2):187-218.
4. Hildebrand M. 1977. Analysis of Asymmetrical Gaits. *J. of Mammalogy* 58(31):131-156.
5. Kubow T. and Full R. 1999. The Role of the Mechanical System in Control: A Hypothesis of Self-stabilization in Hexapedal Runners. *Phil. Trans. R. Soc. of Lond. Biological Sciences* 354(1385):854-862.
6. McGeer T. 1989. *Passive Bipedal Running*. Technical Report, CSS-IS TR 89-02, Centre For Systems Science, Burnaby, BC, Canada.
7. Poulakakis I. 2002. *On the Passive Dynamics of Quadrupedal Running*. M. Eng. Thesis, McGill University, Montréal, QC, Canada.
8. Poulakakis I., Papadopoulos E., Buehler M. 2003. On the Stable Passive Dynamics of Quadrupedal Running. *Proc. IEEE Int. Conf. on Robotics and Automation* (1):1368-1373.
9. Raibert M. H. 1986. *Legged Robots That Balance*. MIT Press, Cambridge MA.
10. Schmiedeler J.P. and Waldron K.J. 1999. The Mechanics of Quadrupedal Galloping and the Future of Legged Vehicles. *Int. J. of Robotics Research* 18(12):1224-1234.
11. Seyfarth A., Geyer H., Guenther M. and Blickhan R. 2002. A Movement Criterion for Running, *J. of Biomechanics* 35:649-655.
12. Talebi S., Poulakakis I., Papadopoulos E. and Buehler M. 2001. Quadruped Robot Running with a Bounding Gait. *Experimental Robotics VII*, D. Rus and S. Singh (Eds.), pp. 281-289, Springer-Verlag.